Nucleic Acids Research, 1995, Vol. 23, No. 8 1333–1340

Evidence for DAPI intercalation in CG sites of DNA oligomer [d(CGACGTCG)]$_2$: a ^{1}H NMR study

Edoardo Trotta*, Ettore D'Ambrosio, Giampietro Ravagnan and Maurizio Paci[1]

Istituto di Medicina Sperimentale, CNR, Viale Marx 15, 00137 Roma, Italy and [1]Dipartimento di Scienze e Tecnologie Chimiche, Universita' di Roma 'Tor Vergata', Roma, Italy

Received January 13, 1995; Revised and Accepted March 1, 1995

ABSTRACT

The interaction between 4',6-diamidino-2-phenylindole (DAPI) and the DNA oligomer [d(CGACGTCG)]$_2$ has been investigated by proton one- and two-dimensional NMR spectroscopy in solution. Compared with the minor groove binding of the drug to [d(GCGATCGC)]$_2$, previously studied by NMR spectroscopy, the interaction of DAPI with [d(CGACGTCG)]$_2$ appears markedly different and gives results typical of a binding mechanism by intercalation. C:G imino proton signals of the [d(CGACGTCG)]$_2$ oligomer as well as DAPI resonances appear strongly upfield shifted and sequential dipolar connectivities between cytosine and guanine residues show a clear decrease upon binding. Moreover, protons lying in both the minor and major grooves of the DNA double helix appear involved in the interaction, as evidenced principally by intermolecular drug–DNA NOEs. In particular, the results indicate the existence of two stereochemically non-equivalent intercalation binding sites located in the central and terminal adjacent C:G base pairs of the palindromic DNA sequence. Different lifetimes of the complexes were also observed for the two sites of binding. Moreover, due to the fast exchange on the NMR timescale between free and bound species, different interactions in dynamic equilibrium with the observed intercalative bindings were not excluded.

INTRODUCTION

The synthetic antibiotic 4',6-diamidino-2-phenylindole (DAPI) (Fig. 1) is one of the most used fluorescent dyes for DNA and chromosomes (1–8). Several papers have elucidated the type of interaction with nucleic acids and it is now generally accepted that DAPI shows at least two primary modes of binding to DNA (9–23). The first mode is mainly characterized by a strong binding affinity, high specificity for AT clusters and a marked increase in DAPI fluorescence quantum yield. The second mode, which is not sequence specific, shows weaker binding affinity than the first one and produces a decrease in DAPI fluorescence quantum yield. While the first type of binding has been characterized by spectroscopic and X-ray studies as a minor groove interaction, the second is still the object of discussion and both intercalation and major groove binding modes have been proposed. The studies of Wilson *et al.* on G:C or mixed base pair sequences indicate an intercalation binding mechanism by analogy with classic intercalators (9–11). Their conclusions are supported by several strands of experimental evidence: unwinding results with supercoiled DNA, viscosimetric and NMR titrations, dissociation kinetics experiments, effects on bleomycin cleavage of DNA and binding studies. On the other hand, in a recent study Kim *et al.* excluded both minor groove and standard intercalation binding of DAPI in poly[d(GC)]$_2$ and proposed an interaction of the drug in the major groove of the polymer (17). Their conclusions are based on the observation that upon binding with poly[d(GC)]$_2$, DAPI molecules show a relatively large accessibility to the I_2 quencher, a decrease in fluorescence intensity and linear dichroism spectra that are compatible only with a major groove binding mechanism. Moreover, they have recently reported that DNA oligomers containing non-contiguous A:T base pairs show the same mode of binding found for GC sequences (16). In this paper we report a NMR study of the interaction of DAPI with [d(CGACGTCG)]$_2$ to elucidate the mode of binding of the drug to DNA sequences that do not contain contiguous A:T base pairs.

MATERIALS AND METHODS

Sample preparation

The DNA oligomers were synthesized with a Gene Assembler Plus (Pharmacia LKB) instrument on the 10 μM scale. After deprotection, the oligonucleotides were purified by extraction with 0.5 vol. chloroform:isoamyl alcohol (24:1) and successively by 2 vol. diethyl ether. Finally, the DNA oligomers in 0.5 M NaCl solution were precipitated by 2 vol. ethanol at –20°C and desalted by chromatography on Sephadex G-10. ^{1}H-NMR spectroscopy was used to evaluate the absence of impurities. The DNA concentration expressed as duplex was determined spectrophotometrically at 260 nm and 80°C (24). DAPI was obtained from Sigma and was used without further purification. The purity of the drug was checked by ^{1}H-NMR and its concentration was measured spectrophotometrically using ε_{342} = 23000/M/cm (3). Samples of free oligonucleotide were suspended in 50 mM NaCl and buffered with 10 mM sodium phosphate at pH 7.00 in 100%

* To whom correspondence should be addressed

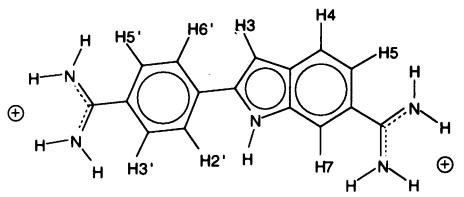

Figure 1. Chemical structure and proton numbering of DAPI.

D_2O. The complexes were prepared by adding concentrated DAPI solution in D_2O to 450 µl buffered volumes of the oligonucleotides. Samples in H_2O were obtained by dissolving lyophilized D_2O solutions in 90% H_2O, 10% D_2O.

NMR spectroscopy

NMR spectra were obtained using Bruker AM 400 and Bruker AMX 600 instruments operating at 400 and 600 MHz respectively. Experiments in D_2O and H_2O solutions were carried out at different temperatures to point out the dependence of spectral features on dynamic processes and to separate overlapping drug and DNA resonances. D_2O and H_2O one-dimensional NMR spectra were run at 400 MHz using a 90° pulse length of 5.8 µs over ~5000 and 10000 Hz spectral widths respectively and accumulated in 16 or 32K of memory with the carrier frequency centered on the water resonance. Resolution enhancements were applied using both the shifted sine-bell and the Lorentz–Gauss transformation. The p.p.m. scale was referenced to tetramethylsilane, assuming residual protonated water HDO as 4.76 p.p.m. Titration experiments were performed by adding small concentrated volumes of drug solution (8 mM) to the DNA sample (0.2 mM in duplex) and, for every drug:duplex ratio, two spectra at different times were acquired to check the stability of the interaction.

Correlation two-dimensional NMR spectra were performed at 400 MHz by using double quantum filtered (DQF) COSY (25), primitive exclusive (PE) COSY (26) and TOCSY with a MLEV-17 pulse sequence to substitute for the spinlock period (27,28). Dipolar through-space interactions were detected at 400 and 600 MHz by NOESY experiments (29) at different mixing times of 60, 250, 300 and 400 ms. Two-dimensional NMR spectra were typically recorded from 400–700 experiments over 2K of memory in phase-sensitive mode using TPPI (30). $\pi/3$ shifted sine-bell or $\pi/2$ shifted squared sine-bell window functions were applied in both directions. Suppression of the water signal in one- and two-dimensional spectra of H_2O samples was obtained with a 1–1 spin echo pulse sequence $90_x - t - 90_{-x} - \Delta - 90_\phi - 2t - 90_{-\phi} - \Delta$–AQ (31). To optimize solvent suppression and the excitation profile of the 1–1 echo sequence, the carrier frequency was adjusted to the water resonance; $\Delta = 50$ µs and $t = 220$ or 80 µs were used for DNA alone or complex respectively. Moreover, a short homospoil (1.5–10 ms) was applied during the mixing time of NOESY experiments.

All data were processed on a Digital VaxStation 2000 graphic terminal using the TRITON NMR software of the NMR Group of the Department of Organic Chemistry, University of Utrecht, The Netherlands (32).

Table 1. Proton chemical shift values (p.p.m.) of DNA octamer $[d(CGACGTCG)]_2$ at 28°C

base	H1'	H2'	H2"	H3'	H4',5',5"	H6/8	H2/5/Me	H1/3*	$H4_a$*	$H4_b$*
					Free DNA					
C1	5.76	1.88	2.38	4.71	4.07,3.72	7.63	5.93		8.37	7.23
G2	5.48	2.74	2.79	5.01	4.32,3.99,4.09	7.98		13.06		
A3	6.28	2.72	2.93	5.07	4.49,4.19,4.23	8.24	7.92			
C4	5.62	2.03	2.38	4.82	4.18,4.27	7.23	5.25		8.26	6.70
G5	5.97	2.61	2.78	4.94	4.37,4.14	7.83		12.83		
T6	6.06	2.10	2.47	4.87	4.23,4.15	7.30	1.41	13.94		
C7	5.75	2.03	2.38	4.85	4.13,4.09	7.52	5.72		8.76	7.24
G8	6.19	2.63	2.38	4.70	4.19,4.08	7.97		13.25		
					2:1 DAPI:duplex complex					
C1	5.64	1.74	2.28	4.64	4.03,3.70	7.49	5.76		8.17	6.97
G2	5.39	2.67	2.71	4.97	4.27,4.05,3.93	7.90		12.85		
A3	6.18	2.64	2.82	5.01	4.39,4.19,4.12	8.16	7.89			
C4	5.61	2.02	2.23	4.77	4.06,4.10	7.18	5.17		8.13	6.62
G5	5.76	2.53	2.66	4.86	4.02,3.90	7.84		12.82,11.74		
T6	5.90	2.03	2.34	4.76	4.00,3.94	7.19	1.33	13.81,13.49		
C7	5.60	1.94	2.24	4.74	3.99,3.94,3.85	7.40	5.62		8.52	7.03
G8	6.02	2.55	2.28	4.62	4.11,4.00	7.82		12.72		

* Chemical shift at 3° C

RESULTS

Resonance assignment and conformation of free $[d(CGACGTCG)]_2$

The assignment of proton resonances of the $[d(CGACGTCG)]_2$ oligomer was performed by following the well-established procedures described in the literature (33–39). NOESY spectra at long mixing times (250–300 ms) were used for the sequential assignments of H6, H8, CH_3, H2′ and H2″. The other resonances of deoxyribose spin systems were assigned by a combined analysis of NOESY, TOCSY and DQF COSY spectra. H5 resonances of cytosines were identified by strong scalar and dipolar contacts with the intranucleotide H6 protons. The H4 amino proton resonances of cytosines were assigned from the intranucleotide NOE to H5 resonances. The H1 imino resonances of guanines were identified from interstrand dipolar contacts with cytosine amino groups and, finally, imino proton T6H3 was assigned from its NOE to the H2 proton of A3. The correct assignment of imino protons was supported by their sequential NOEs. Guanine and thymine amino protons were not assigned. The chemical shifts and the individual assignments of the $d(CGACGTCG)]_2$ proton resonances are reported in Table 1.

The conformation of the DNA octamer was evaluated as already described (21), by considering the intensities of intra- and internucleotide NOEs, measured from NOESY spectra acquired with a 60 ms mixing time, and the values of vicinal coupling constants of deoxyribose ring protons measured either by analysis of cross-peak fine structures in the PE COSY spectrum or, directly, in resolution-enhanced one-dimensional NMR spectra (26,40–44). NOE intensities (Fig. 2A), as well as the values of vicinal coupling constants ($7.9 < {}^3J_{1'-2'} < 10.2$, $5 < {}^3J_{1'-2''} < 6.4$ and, excluding G8, ${}^3J_{2''-3'} < 2$), clearly indicate that the conformation of $[d(GCGATCGC)]_2$ belongs to the general B-type family. The possible existence of a single-stranded form or left-handed conformation of the double-stranded DNA were ruled out by the observation of NOESY cross-peaks between guanine H1 and cytosine H4 and very weak or no intranucleotide NOEs between H1′ and H8 resonances of purines in NOESY spectra at short mixing times respectively.

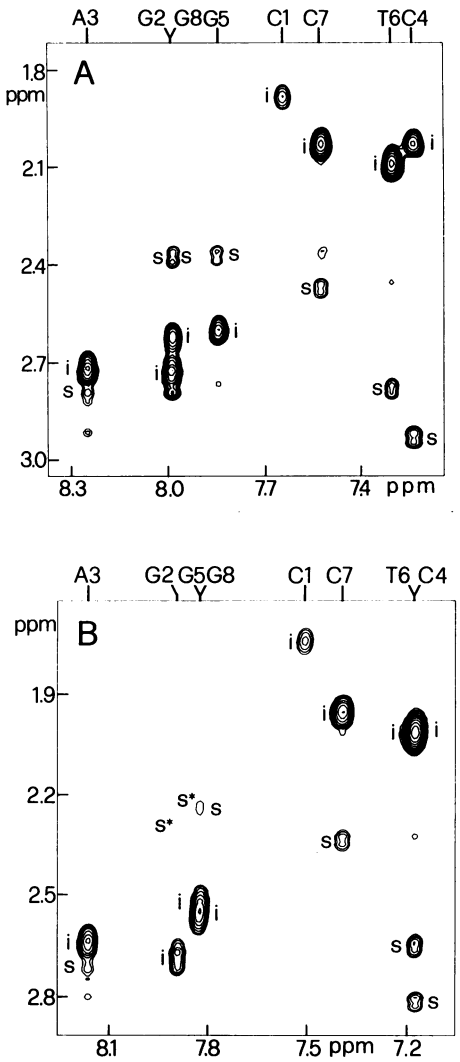

Figure 2. Expanded region of NOESY spectra of $[d(CGACGTCG)]_2$ (**A**) and a DAPI–$[d(CGACGTCG)]_2$ = 2:1 complex (**B**) in a D_2O solution, acquired with a mixing time of 60 ms at 28°C. The position of intranucleotide H6/8(i)–H2′(i) and sequential H6/8(i)–H2″(i-1) cross-peaks are labelled by i and s respectively. s* indicates the position of sequential cross-peaks that are absent in the spectrum of the complex due to the interaction.

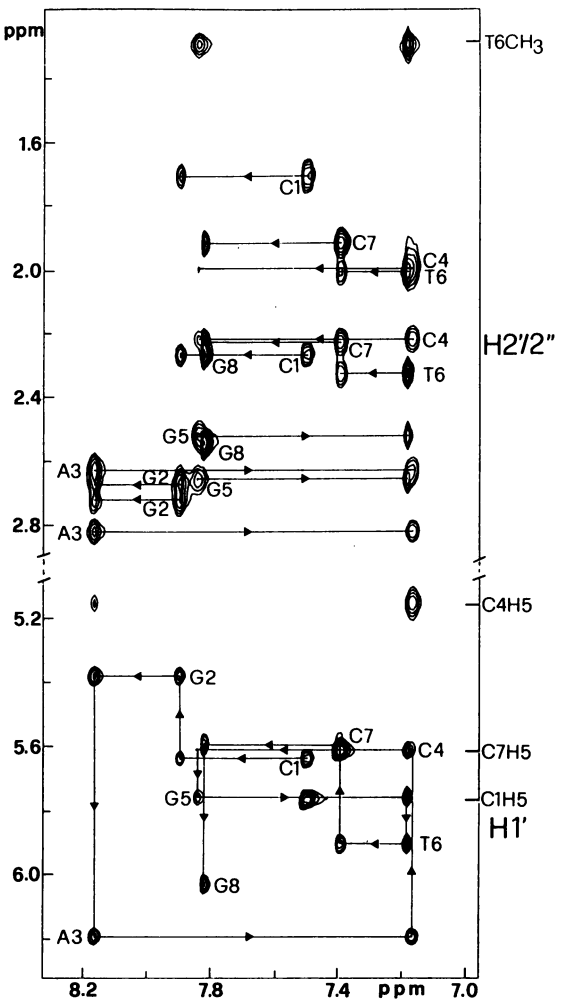

Figure 3. Expanded region of a 600 MHz NOESY spectrum of a DAPI–$[d(CGACGTCG)]_2$ = 2:1 complex recorded in a D_2O solution, at 28°C with a mixing time of 300 ms. The arrows show the DNA sequential assignment via H6/8–H2′/2″ (upper region) and H6/8–H1′ (lower region) with intraresidue cross-peaks indicated by labels. To point out low intensities of 5′-C4G5-3′ sequential connectivities high levels of the contour plot are shown.

Resonance assignment and DNA conformation in the DAPI–$[d(CGACGTCG)]_2$ complex

The spectral behavior of DNA resonances in titration experiments with DAPI indicates that free and bound species at 26°C are in a fast or moderately fast exchange on the NMR timescale. Moreover, the resonances of non-labile DNA protons upon addition of DAPI show slight broadening, with the exception C4H1′ and C4H5, which appear sensitively broadened also at low DAPI:duplex ratios. Due to the low intensity of the broad DAPI resonances we focused our study on the DAPI:duplex ratio 2:1, rather than a DAPI:duplex ratio of 1:1. Complexes with a DAPI:duplex ratio more than ~2 were not stable and the drug in excess, which appeared insoluble, was eliminated by centrifugation. Due to the dynamics of the interaction, the 400 MHz instrument was preferred to the 600 MHz instrument for the study of intermolecular interactions.

The DNA resonances in the complex were assigned by the same procedure reported for DNA alone and by following changes in titration experiments. Figure 3 shows the sequential assignment of DNA resonances in the complex using NOE connectivities between base H6/H8 and H1′/H5/H2′/H2″/Me. The complete assignment of the resonances is reported in Table 1.

The B-type conformation of $[d(CGACGTCG)]_2$ does not appear strongly altered upon binding with DAPI. In fact, $^3J_{1'-2'}$, $^3J_{1'-2''}$ and $^3J_{2''-3'}$ vicinal coupling constants do not show changes; only those related to the C4 nucleotide were not measured due to the large linewidth of the C4H1′ signal. As shown in the spectra of Figure 2, no variations were evident for all the intranucleotide dipolar connectivities between H6/8 and H2′. However, sequential NOE connectivities between H2″ and H6/8 resonances clearly appear weak in 5′-C1G2-3′, 5′-C4G5-3′ and 5′-C7G8-3′. This effect of binding was particularly evident in the case of 5′-C4G5-3′

and was also clearly observed in the NOESY spectrum acquired with a mixing time of 300 ms (Fig. 3).

All the DAPI resonances in the complex at 26°C show exchange dynamics in the fast–intermediate range and appear strongly upfield shifted and broadened upon binding. The assignment of the proton chemical shifts of the drug resonances in the complex was performed as already described (21). The H7 indole resonance was identified from its NOE to the NH indole resonance and from scalar long-range interaction with H5 observed in TOCSY experiments. As previously observed for free (11) and minor groove-bound DAPI (21), the drug resonances H3′ and H5′, as well as H2′ and H6′ of the phenyl ring, were not resolved. Therefore, due to overlapping of the H3′ and H5′ as well as H2′, H6′ and H7 DAPI resonances, we refer to H3′/5′ and H2′/6′/7 to indicate these two groups of unresolved resonances at 7.55 and 7.49 p.p.m. respectively. Indole H3, H4, H5 and NH resonances were assigned at 6.55, 7.23, 7.05 and 10.90 p.p.m. respectively. Finally, an exchangeable proton resonance at 8.76 p.p.m., showing NOE contacts only with the unresolved resonance H2′/6′/7, was tentatively assigned to the NH_2 protons of the DAPI indole group.

NMR of exchangeable protons of the DAPI–[d(CGACGTCG)]$_2$ complex

One- and two-dimensional spectra of exchangeable protons were performed at 400 MHz and the resonances were assigned from the analysis of NOESY spectra acquired at 7, 12 and 26°C. As reported for DNA alone, the assignment was performed by following NOE connectivities between cytosine amino groups and both intranucleotide H5 and interstrand guanine imino resonances. The thymine imino resonance was assigned from its strong interstrand NOE to the A3H2 resonance. The results were checked by a comparative analysis with the free [d(CGACGTCG)]$_2$ and by following the temperature changes of imino proton signals. The assignments are reported in Table 1.

Upon binding with DAPI, the resonances due to imino protons of DNA appear strongly perturbed. As can be seen from the spectra of Figure 4, at 40°C only the imino proton resonances of G2, G5 and T6 are observable. Due to the thermally induced end fraying of the double helix, the G8H1 signal is lost and becomes easily observable only at lower temperatures. With the exception of G8H1, the spectrum at 40°C clearly shows that the linewidths of the imino proton resonances increase from the ends to the center of the oligonucleotide sequence: G2H1 < T6H3 < G5H1. This effect cannot be simply attributed to a different rate of chemical exchange with water protons. In fact, lowering the temperature causes first a broadening of T6H3 and G5H1 resonances and then, at 7.5°C, splitting of each of these resonances into two slow exchanging resonances that become sharper and sharper as the temperature is further lowered. Therefore, this effect of binding on the linewidth of the imino resonances is prevalently caused by the rate of exchange and the size of the chemical shift change between the free and bound species. At 3°C the upfield resonance at 11.74 p.p.m. of G5H1, as well as the resonance of T6H3 at 13.49 p.p.m. of the complex, show marked upfield shifts of about 1 and 0.5 p.p.m. respectively, compared with the respective resonances of the free DNA. A marked upfield shift was also observed for the G8H1 resonance (~0.5 p.p.m.) but, differently from the G5H1 and T6H3 resonances, no splitting was evident in the same range of temperature.

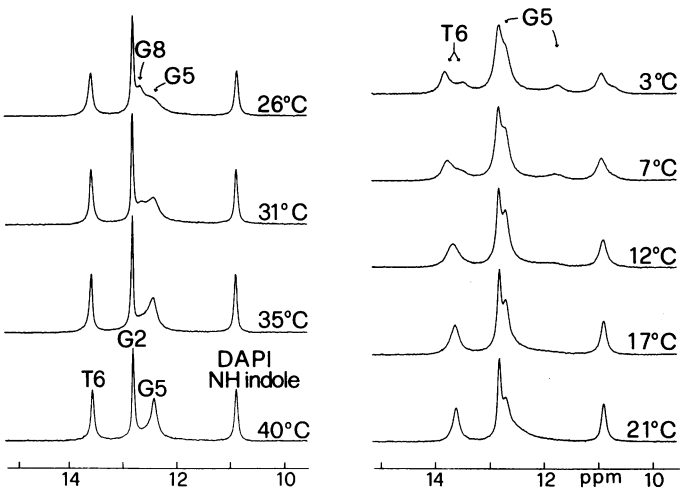

Figure 4. Imino proton spectra of DAPI–[d(CGACGTCG)]$_2$ = 2:1 at various temperatures. The spectra were obtained with a 1–1 spin echo sequence to suppress the water resonance, as reported under Materials and Methods.

Considering that no resonance of the G8H1 free form is observed at both 1:1 and 2:1 DAPI:duplex ratios and that the resonance is further shifted upfield as the ratio is increased from 1:1 to 2:1, we conclude that the dynamics of binding is a fast exchange regime for G8H1. The G2H1 imino resonance appears less perturbed upon binding. This resonance is relatively sharp, upfield shifted ~0.2 p.p.m. and no splitting was observed upon change of temperature.

Drug–DNA intermolecular dipolar contacts

The analysis of NOESY spectra of the complex shows a number of dipolar connectivities between drug and DNA protons. Owing to the line broadening of DAPI resonances and the overlapping of both drug and DNA resonances, the assignment of NOESY cross-peaks was not always unambiguous. The strongest intermolecular NOEs and the only ones observed in the NOESY experiments at short mixing time (60 ms) were found between H5 and H3′/H5′ resonances of DAPI and H4′/5′/5″ resonances of DNA, as shown in Figure 5 (peaks 4 and 5 respectively). The analysis of the NOESY spectra at different temperatures led us to exclude strong interactions of DAPI protons with H4′/5′/5″ of C1, G2 and A3 nucleotides, whereas correlations with at least one resonance of H4′/5′/5″ of G8 as well as G5 can be assigned safely. In NOESY spectra at long mixing times (400 ms), intermolecular NOEs were also observed between the H3′/H5′ resonance of DAPI and the DNA resonances of C7H2″ and C1H2″ (peak 2 in Fig. 5), MeT6 (peak 1 in Fig. 5), G5H8 and G8H8 (peaks marked A in Fig. 6) and the overlapping resonances T6H6/C4H6 (peak B in Fig. 6) and C7H1′/C4H1′ (peak 6 in Fig. 5). The C7H1′/C4H1′, C7H2″, C1H2″ and T6H6/C4H6 DNA resonances show NOEs also to the H5 and H2′/6′/7 DAPI resonances (peaks 6, 7, 2 and 3 of Fig. 5 and peaks B and C of Fig. 6). Moreover, a weak NOE was found between DNA T6H1′ and DAPI H2′/6′/7 (peak 8 in Fig. 5). NOESY spectra, carried out in H_2O solution at 12°C and with a mixing time of 210 ms, show intermolecular NOE between the NH indole resonance of DAPI and DNA resonances assigned to the C1H4$_b$ and C4H4$_b$ amino protons (peaks A and B in Fig. 7 respectively). Furthermore, as can be seen from the spectrum of Figure 7, the DAPI NH indole resonance shows NOESY cross-peaks with the overlapping

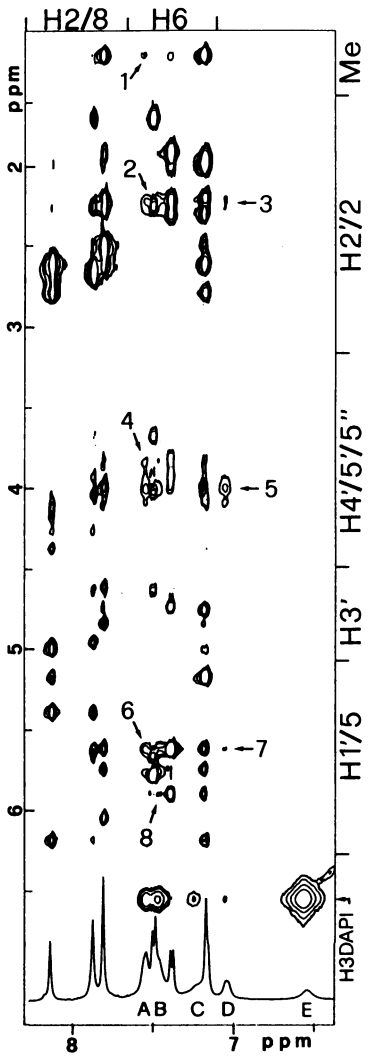

Figure 5. Expanded region of a 400 MHz NOESY spectra of a DAPI–[d(CGACGTCG)]$_2$ = 2:1 complex in a D_2O solution, acquired with a mixing time of 400 ms at 31°C. DAPI resonances are labeled by letters: H3′/5′ (A), H2′/6′/7 (B), H4 (C), H5 (D) and H3 (E). Arrows labeled by numbers indicate intermolecular DAPI–DNA NOEs: H3′/5′–MeT6 (1), H3′/5′–C7H2″ (2), H3′/5′–C1H2″ (2), H2′/6′/7–C7H2″ (2), H2′/6′/7–C1H2″ (2), H5–C1H2″ (3), H5–C7H2″ (3), H3′/5′–H4′/5′/5″ (4), H2′/6′/7–H4′/5′/5″ (4), H5–H4′/5′/5″ (5), H3′/5′–C4H1′/C7H1′ (6), H2′/6′/7–C4H1′/C7H1′ (6), H5–C4H1′/C7H1′ (7), H2′/6′/7–T6H1′ (8).

C4H1′/C7H1′ DNA resonances (peak C) and with resonances that fall in the H4′/5′/5″ and H2′/2″ regions of the DNA spectrum (peaks D and E in Fig. 7). The assignment of these last DNA resonances to the respective nucleotides was not feasible, because of broadening and consequent overlap of the resonances due to the low temperature of the experiments.

DISCUSSION

Effects of binding on DAPI resonances

It has been reported that DAPI exhibits at least two different modes of binding to DNA that are easily distinguished one from the other by a marked difference in the chemical shift of the drug proton NMR resonances. The first mode is found to be a minor groove

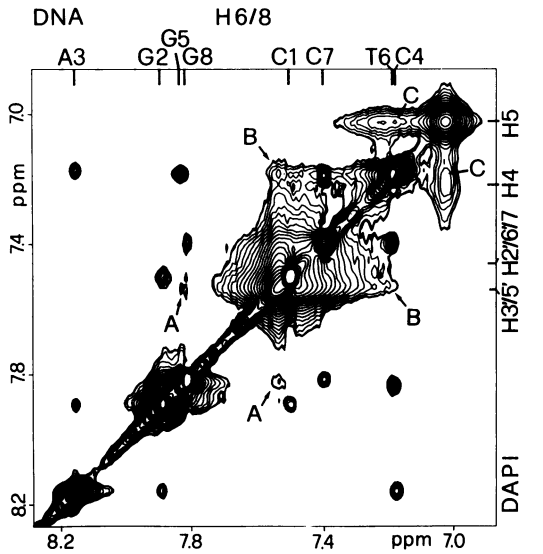

Figure 6. Expanded region of a 600 MHz NOESY spectra of a DAPI–[d(CGACGTCG)]$_2$ = 2:1 complex in a D_2O solution, acquired with a mixing time of 400 ms at 28°C. The arrows indicate intermolecular DAPI–DNA NOEs: H3′/5′–G5H8 and H3′/5′–G8H8 (A), H3′/5′–C4H6/T6H6 (B), H2′/6′/7–C4H6/T6H6 (B), H5–C4H6/T6H6 (C).

binding and is shown to cause a slight downfield shift of DAPI resonances in DAPI–poly[d(AT)]$_2$ (10) and DAPI–[d(GCGATCGC)]$_2$ complexes (21). In contrast, large upfield shifts, attributed to an effect of intercalation, were observed in complexes of DAPI with sonicated poly[d(GC)]$_2$ (11).

In the complex examined in this work, between DAPI and [d(CGACGTCG)]$_2$, the drug resonances exhibit large upfield shifts that are consistent with a mechanism of interaction similar to that observed for poly[d(GC)]$_2$ complexes. Thus, single A:T base pairs isolated in G:C sequences, as in [d(CGACGTCG)]$_2$, do not allow minor groove binding of the drug as observed in the complex with the [d(GCGATCGC)]$_2$ sequence containing two contiguous A:T base pairs (21). This finding is consistent with spectrophotometric results previously reported for binding of DAPI with oligonucleotides containing a variable number of contiguous A:T base pairs (16) and alternating DNA polymers poly(dAC)·poly(dGT) and poly(dAG)·poly(dCT) (9–11,23).

The strong upfield shift of the drug resonances was also observed in our preliminary studies of binding of DAPI with single-stranded DNA oligomers (data not shown). This result demonstrates that the presence of intact grooves of double-stranded DNA is not necessary for upfield shifting of the drug resonances and suggests that intercalation or an external backbone interaction, but not groove binding, could be the DAPI mode of binding with single-stranded as well as double-stranded DNA without contiguous A:T base pairs.

Effects of binding on [d(CGACGTCG)]$_2$ resonances

All the proton resonances of [d(CGACGTCG)]$_2$ appear upfield or non-shifted upon binding with the drug. In the minor groove binding of DAPI with [d(GCGATCGC)]$_2$ previously reported (21), the strongest shifts of DNA resonances were observed for protons lying in the minor groove. In contrast, in the complex examined in this work, the strongest upfield shifts were observed for the resonances of imino protons.

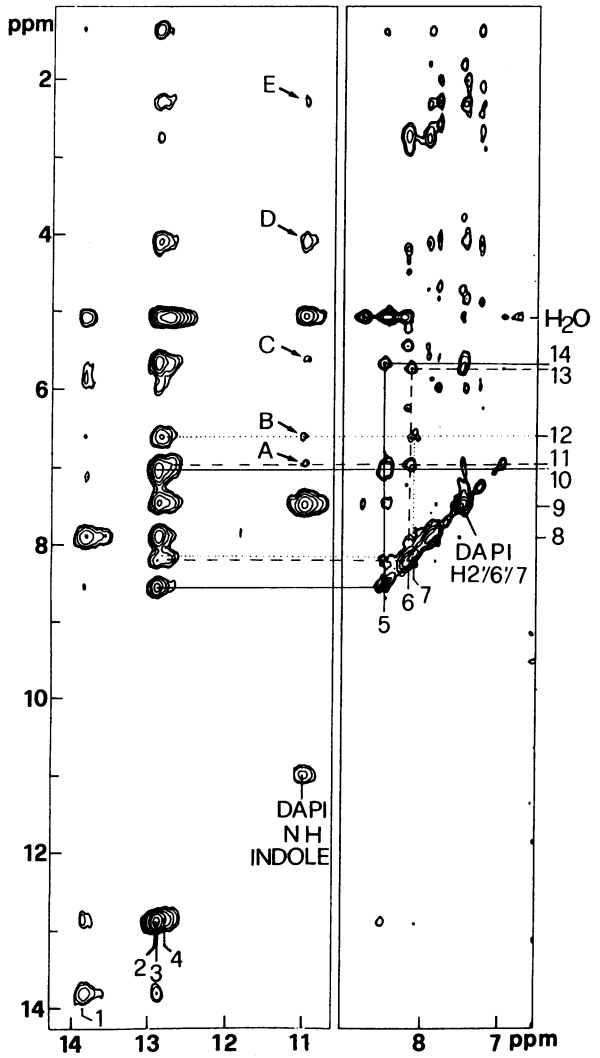

Figure 7. Expanded region of the NOESY spectra of a DAPI–[d(CGACGTCG)]$_2$ = 2:1 complex in 90% H_2O, 10% D_2O, acquired with a mixing time of 210 ms at 12°C. The numbers indicate the position of relevant DNA resonances: T6H3 (1), G2H1 (2), G5H1 (3), G8H1 (4), C7H4$_a$ (5), C1H4$_a$ (6), C4H4$_a$ (7), A3H2 (8), C7/C1H6 (9), C7H4$_b$ (10), C1H4$_b$ (11), C4H4$_b$ (12), C1H5 (13), C7H5 (14). The lines show the correlations followed to assign G:C labile protons: G2H1–C7H4$_{(a \text{ and } b)}$–C7H5 (solid line), G5H1–C4H4$_{(a \text{ and } b)}$ (dotted line) and G8H1–C1H4$_{(a \text{ and } b)}$–C1H5 (broken line). The letters indicate intermolecular NOEs of the NH indole of DAPI to DNA resonances as follows: C1H4$_b$ (A), C4H4$_b$ (B), C4H1'/C7H1' (C), H4'/5'/5'' (D) and H2'/2'' (E).

As expected in the case of intercalation of DAPI molecules in the central couple of base pairs C4:G5, a strong reduction of sequential NOEs between G5H8 and C4 deoxyribose protons and a strong upfield shift of about 1 p.p.m. of the G5H1 resonance were observed (45). Moreover, C4H1', as well as C4H5, appear markedly broadened compared with the other non-labile proton resonances of DNA. Since this effect involves protons of C4 exposed in the minor and major groove and is to be attributed to a large difference in the chemical shift between the free and bound forms, this is also consistent with intercalation of the drug in the central couple of base pair C4:G5.

At low temperature the integrated intensity of the upfield resonance of G5H1 shows the same value as measured for the upfield resonance of T6H3. This suggests that the shift of the T6 imino resonance (~0.5 p.p.m.) has to be attributed to an effect of the near 5'-C4G5-3' intercalation site. Such an effect was also observed with the classic intercalator ethidium bromide (46).

The strong upfield shift of the G8H1 resonance and the low intensity of sequential NOEs between the protons of C1 and G2 and C7 and G8 indicate that the last two base pairs at the ends of the palindromic oligomer are also sites of intercalation. The presence of this second binding site is supported by another observation. In the complex at temperatures below 7°C G8H1 shows a single averaged resonance, while two separate slow exchanging resonances appear for both the T6 and G5 imino protons. Since the difference in chemical shifts between free and bound species is higher for G8H1 ($\delta_{bound} - \delta_{free} > 212$ Hz) than T6H3 ($\delta_{bound} - \delta_{free} = 180$ Hz), these different effects cannot be due to a single binding of the drug to the DNA oligomer. Therefore, we conclude that DAPI binds [d(CGACGTCG)]$_2$ in at least two different sites with different exchange rates. The first binding causes the most evident effects on the imino chemical shifts of the central base pairs of the DNA octamer and shows a slow exchange rate on the NMR timescale. The second causes a major alteration in the imino chemical shift of the terminal base pairs and exhibits a faster exchange rate than the first one. The thermally induced instability of the double helix in correspondence with the extreme base pair C1:G8, as indicated by the fast exchange of its imino proton with water, explains the relatively weak influence of this last interaction on the G2H1 resonance, which appears less upfield shifted and narrower than the G5H1 resonance.

Intermolecular NOEs

The intermolecular NOEs observed between the drug and the DNA protons are also consistent with an intercalation binding mechanism. The possibility that DAPI binds the oligomer only in the major groove was ruled out by the evidence that phenyl and indole groups of the drug are exposed in the minor groove of the DNA oligomer. This is shown by the strong NOEs observed between DAPI protons H3'/5' and H5 and DNA protons H4'/5'/5'' that lie in the minor groove. Such NOEs appear the strongest intermolecular dipolar contact between the drug and DNA and the only ones observed in NOESY spectra acquired with a short mixing time (60 ms). In agreement with intercalative binding of the drug at the central and terminal 5'-CG-3' bases, several intermolecular NOEs involving DNA protons of the C4:G5, C7:G2 and C1:G8 base pairs that are exposed in both the grooves were observed.

However, a fine evaluation of the structure of the complex from intermolecular NOEs was precluded by the resolution of the spectra and the dynamics of the interaction. In particular, several intermolecular NOEs were not assigned to individual protons, due to the broadening and overlapping of drug and DNA resonances. This appears particularly evident for all the NOEs involving drug protons of the phenyl ring or H7 of the indole group, which were not unambiguously assigned. Furthermore, the moderately short lifetime of the interaction causes both a large broadening of the drug resonances and a decrease in the effective time of intermolecular contacts with respect to the nominal mixing time of the NOESY experiments. Both these effects strongly reduced the intensities of DAPI–DNA NOEs. Almost all the intermolecular NOEs were observed only at long mixing

times, where non-negligible effects of spin diffusion on NOE intensities occur. In addition, since the free and bound species are in fast exchange on the NMR timescale, the free rotation of the phenyl ring around the phenyl–indole bond, which occurs in free DAPI (10), has to be considered. This rotation alternatively brings H2′ or H6′ near to the H3 and NH indole protons and NOEs between DNA and these phenyl protons can be transferred to the other side of the drug molecule as a combined effect of rotation and spin diffusion. This argument explains the fact that the NH indole resonance of DAPI shows NOE to the overlapping DNA resonances of C4H1′ and C7H1′, as well as H4′/5′/5″, protons exposed in the minor groove and the resonances of H2′/2″, C1H4 and C4H4 protons that belong to the major groove. However, we cannot exclude the possibility that these effects could also be due to another binding mechanism in dynamic equilibrium with the intercalated molecules.

A molecular modeling of DAPI intercalated at a CG site of DNA has been proposed by Wilson *et al.* (10), in which they also discuss the effects of intercalation on the NMR resonances of DAPI. In the model the H5 and H5′ of DAPI are oriented towards the H5′ protons of DNA, in agreement with our findings obtained with NOEs at short mixing time.

CONCLUSION

Our study shows that DAPI binds the DNA oligomer $[d(CGACGTCG)]_2$ by intercalation in the 5′-CG-3′ sites of the oligonucleotide. The results of this work can be summarized in the following points.

(i) The effects of binding on the$[d(CGACGTCG)]_2$ and DAPI spectra appear markedly different from that observed on minor groove binding of the drug with $[d(GCGATCGC)]_2$ previously reported.
(ii) A mechanism of binding of the drug only in the major groove is excluded by the strong NOE contacts between the drug and minor groove protons of the oligonucleotide.
(iii) The shift of DAPI and $[d(CGACGTCG)]_2$ resonances are characteristic of intercalative ligand binding.
(iv) The upfield shift of DAPI resonances observed in the binding with single-stranded DNA appears very similar to that observed in the complex with $[d(CGACGTCG)]_2$, suggesting that groove binding is not responsible for such marked upfield shifts.
(v) Intercalative binding of the drug at the 5′-C4G5-3′ site is supported by intermolecular NOEs, weakening of sequential NOEs between the G5 base and C4 deoxyribose protons, strong upfield shifting of the G5 imino resonance and broadening of the H1′ and H5 resonances of C4.
(vi) Intercalative binding of the drug between the C1:G8 and G2:C7 base pairs is supported by intermolecular NOEs, weakening of sequential NOEs between the two terminal base pairs and strong upfield shifting of the G1 imino resonances.
(vii) The presence of two binding sites located in the central and terminal regions of the oligonucleotide sequence is also supported by dynamic results.
(viii) Short mixing time NOEs agree with the orientation of the H5 and H5′ of DAPI towards minor groove H5′ protons of DNA, as reported in the model of intercalation proposed by Wilson *et al.* (10).

ACKNOWLEDGEMENTS

We thank Dr Daniela Orru' for helpful discussions and Mr Fabio Bertocchi and Enrico Rossi for technical assistance with the 400 and 600 MHz instruments. The NMR Service of the CNR Research Area of Montelibretti, Roma, courtesy of A. L. Segre, is gratefully acknowledged for running the 600 MHz experiments.

REFERENCES

1 Latt,S.A. (1976) *Annu. Rev. Biophys. Bioengng*, **5**, 1–37.
2 Lee,G.M., Thornthwaite,J.T. and Rasch,E.M. (1984) *Anal. Biochem.*, **137**, 221–226.
3 Kapuscinski,J. and Skoczylas,B. (1977) *Anal. Biochem.*, **83**, 252–257.
4 Kapuscinski,J. and Yanagi,K. (1979) *Nucleic Acids Res.*, **6**, 3535–3542.
5 Naimski,P., Bierzynski,A. and Fikus,M. (1980) *Anal. Biochem.*, **106**, 471–475.
6 Cavatorta,P., Masotti,L. and Szabo,A.G. (1985) *Biophys. Chem.*, **22**, 11–16.
7 Brunk,C.F., Jones,K.C. and James,T.W. (1979) *Anal. Biochem.*, **92**, 497–500.
8 Williamson,D.H. and Fennel,D.J. (1975) *Methods Cell Biol.*, **12**, 335–351.
9 Wilson,W.D., Tanious,F.A., Barton,H.J., Jones,R.L., Fox,K., Wydra,R.L. and Strekowski,L. (1990) *Biochemistry*, **29**, 8452–8461.
10 Wilson,W.D., Tanious,F.A., Barton,H.J., Wydra,R.L., Jones,R.L., Boykin,D.W. and Strekowski,L. (1990) *Anti-cancer Drug Design*, **5**, 31–42.
11 Wilson,W.D., Tanious,F.A., Barton,H.J., Strekowski,L. and Boykin,D.W. (1989) *J. Am. Chem. Soc.*, **111**, 5008–5010.
12 Kubista,M., Åkerman,B. and Nordén,B. (1987) *Biochemistry*, **26**, 4545–4553.
13 Manzini,G., Barcellona,M.L., Avitabile,M. and Quadrifoglio,M. (1983) *Nucleic Acids Res.*, **11**, 8861–8876.
14 Larsen,T.A., Goodsell,D.S., Cascio,D., Grzeskowiak,K. and Dickerson, R.E. (1989) *J. Biomol. Struct. Dyn.*, **7**, 477–491.
15 Loontiens,F.G., McLaughlin,L.W., Diekmann,S. and Clegg,R.M. (1991) *Biochemistry*, **30**, 182–189.
16 Jansen,K., Nordén,B. and Kubista,M. (1993) *J. Am. Chem. Soc.*, **115**, 10527–10530.
17 Kim,S.,K., Eriksson,S., Kubista,M. and Nordén,B. (1993) *J. Am. Chem. Soc.*, **115**, 3441–3447.
18 Sehlstedt,U., Kim,S.K. and Nordén,B. (1993) *J. Am. Chem. Soc.*, **115**, 12258–12263.
19 Mohan,S. and Yathindra,N. (1994) *J. Biomol. Struct. Dyn.*, **11**, 849–867.
20 Tanious,F.A., Veal,J.M., Buczak,H., Ratmeyer,L.S. and Wilson,W.D. (1992) *Biochemistry*, **31**, 3103–3112.
21 Trotta,E., D'Ambrosio,E., Del Grosso,N., Ravagnan,G., Cirilli,M. and Paci,M.(1993) *J. Biol. Chem.*, **268**, 3944–3951.
22 Eriksson,S., Kim,S.K., Kubista,M. and Nordén,B.(1993) *Biochemistry*, **32**, 2987–2998.
23 Kapuscinski,J. and Szer,W. (1979) *Nucleic Acids Res.*, **6**, 3519–3534.
24 Cantor,C., Warshaw,M.W. and Shapiro,H. (1970) *Biopolymers*, **9**, 1059–1077.
25 Rance,M., Sørensen,O.W., Bodenhausen,G., Wagner,G., Ernst,R.R. and Wüthrich,K. (1983) *Biochem. Biophys. Res. Commun.*, **117**, 479–485.
26 Mueller,L. (1987) *J. Magn. Resonance*, **72**, 191–196.
27 Bax,A. and Davis,D.G. (1986) *J. Magn. Resonance*, **65**, 355–360.
28 Braunschweiler,L. and Ernst,R.R. (1983) *J. Magn. Resonance*, **53**, 521–528.
29 Jeener,J., Meier,B.H., Bachmann,P. and Ernst,R.R. (1979) *J. Chem. Phys.*, **71**, 4546–4553.
30 Marion,D. and Wutrich,K. (1983) *Biochem. Biophys. Res. Commun.*, **113**, 967–974.
31 Sklenar,V. and Bax,A. (1987) *J. Magn. Resonance*, **74**, 469–479.
32 Boelens,R. and Vuister,G. (1990) Software for processing multidimensional NMR spectra. Courtesy of Professor R.Kaptein, Utrecht, The Netherlands.
33 Clore,G.M. and Gronenborn,A.M. (1985) *FEBS Lett.*, **179**, 187–192.
34 Hare,D.R., Wemmer,D.E., Chou,S.H., Drobny,G. and Reid,B.R. (1983) *J. Mol. Biol.*, **171**, 319–336.

35 Hosur,R.V., Ravikumar,M., Roy,K.B., Zu-Kun,T., Miles,H.T. and Govil,G. (1985) In Govil,G., Khetrapal,C.L. and Saran,A. (eds), *Magnetic Resonance in Biology and Medicine*. Tata McGraw-Hill, New Delhi, India, pp. 243–260.
36 Reid,D.G., Salisbury,S.A., Bellard,S., Shakked,Z. and Williams,D.H. (1983) *Biochemistry*, **22**, 2019–2025.
37 Scheek,R.M., Russo,N., Boelens,R., Kaptein,R. and van Boom,J.H. (1983) *J. Am. Chem. Soc.*, **105**, 2914–2916.
38 Scheek,R.M., Boelens,R., Russo,N., van Boom,J.H. and Kaptein,R. (1984) *Biochemistry*, **23**, 1371–1376.
39 Boelens,R., Sheek,R.M., Dijkstra,K. and Kaptein,R. (1985) *J. Magn. Resonance*, **62**, 378–386.
40 Wüthrich,K. (1986) *NMR of Proteins and Nucleic Acids*. John Wiley & Sons, New York, NY, pp. 203–255.
41 Patel,D.J.,Shapiro,L. and Hare,D. (1987) *Q. Rev. Biophys.*, **20**, 35–112.
42 Hosur,R.V., Govil,G. and Miles,H.T. (1988) *Magn. Resonance Chem.*, **26**, 927–944.
43 Altona,C. (1982) *Recl. Trav. Chim. Pays-Bas.*, **101**, 413–433.
44 Davies,D.B. (1978) *Prog. NMR Spectrosc.*, **12**, 135–225.
45 Feigon,J., Denny,W.A., Leupin,W. and Kearns,D.R. (1984) *J. Med. Chem.*, **27**, 450–465.
46 Patel,D.J. and Canuel,L.L. (1976) *Proc. Natl. Acad. Sci. USA*, **73**, 3343–3347.